ACS OMEGA

Article

Oil Recovery Efficiency and Mechanism of Low Salinity-Enhanced Oil Recovery for Light Crude Oil with a Low Acid Number

Abhijit Kakati, Ganesh Kumar, and Jitendra S. Sangwai*

Read Online

ACCESS | Metrics & More | Article Recommendations | Supporting Information

ABSTRACT: Low salinity waterflooding (low salinity-EOR) has attracted great interest from many giant oil producers and is currently under trial in some of the oil fields of the United States, Middle Eastern countries, and North Sea reservoirs. Most of the reported studies on this process were carried out for medium to relatively heavy oil with significant polar contents. In this work, we have investigated low salinity waterflooding performance for light paraffinic crude oil with a low acid number. This study has been performed using crude oil from an Indian offshore oilfield and Indian offshore seawater. Oil recovery efficiencies of seawater and its diluted versions (low salinity seawater) were evaluated through core-flooding experiments performed on a silica sand pack containing small amounts (2 wt %) of bentonite clay saturated with crude oil. Interfacial tension and wettability studies were performed to understand the associated low salinity effects on the crude oil/brine/rock properties. Effluent brine produced during the flooding experiments was also analyzed to obtain a clearer insight into the low salinity-enhanced oil recovery (EOR) mechanism. The results showed that injection of low salinity seawater can significantly increase the waterflood recovery in comparison with high salinity seawater injection. Interfacial tension and contact angle studies revealed that there is an optimum dilution level at which the interfacial tension and wettability are the most favorable for enhanced oil recovery even in the case of light paraffinic crude. These results are in line with the results obtained from the core-flooding experiments. The possible reason behind recovery improvement based on the interfacial tension and wettability studies in conjugation with the effluent brine analysis has been discussed in detail. In this study, we have observed that the enhanced oil recovery efficiency could be achieved by applying low salinity seawater flooding even in the case of light paraffinic oil with a low acid number.
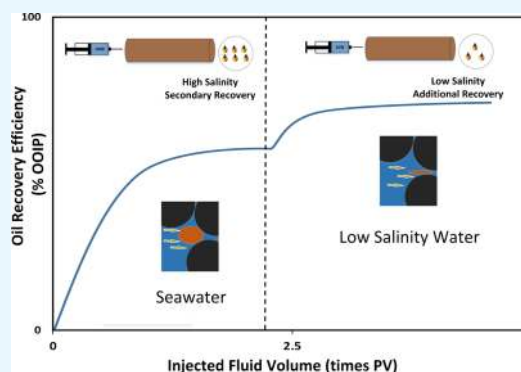
1. INTRODUCTION

Waterflooding is the most common and widely used oil recovery method practiced by the oil industry since 1930s. Conventionally, waterflooding was considered as a physical oil recovery process that serves two primary functions: (1) to maintain reservoir pressure and (2) to displace oil from the reservoir pore space toward the producing well by viscous forces. However, the residual oil saturation left after water-flooding is always found to be high. The fact is that the researchers have not yet understood the waterflooding process well enough from the physicochemical point of view.[1] The research work by the Petrophysics and Surface Chemistry Research Group at the University of Wyoming has pointed out that the injection-water salinity can play a vital role in the oil recovery performance by the waterflooding process.[2−5] In recent years, extensive research work carried out by different groups has indicated that injecting low salinity water can result in a higher oil recovery as compared to conventional high salinity waterflooding. This method is currently under extensive research and has drawn attention of major oil-producing industries in recent times. The outcome of rigorous laboratory investigations has convinced various oil majors (e.g.,

BP, Total, Statoil, Shell, and Saudi Aramco) to implement low salinity-enhanced oil recovery (low salinity-EOR) trial at the field scale.[6−12] As per the data reported in the available literature, low salinity water can reduce the residual oil saturation significantly, even up to 15% in most cases.[11]

A lot of effort has been devoted in the past two decades to understand the mechanism behind the improved oil recovery performance of the low salinity-EOR, viz., (1) formation of fine migration, (2) interfacial tension (IFT) reduction as a result of in-situ saponification, (3) wettability alteration by multi-ion exchange, (4) pH-induced wettability alteration, (5) double-layer expansion, (6) formation of microemulsion, and so forth. Despite several hypotheses presented in the literature, many questions still remain unanswered. Without a clear under-standing of the physicochemical pore-level mechanism, the key parameters or the screening criterion for low salinity-EOR are

difficult to identify. In general, the reservoir mineralogy and crude oil composition are considered to be the important parameters for this process as proposed by various investigators. For example, in some studies, reservoir rock mineralogy has been investigated in detail to understand its importance in low salinity-EOR performance.[1,13−16] Some researchers claimed that the low salinity-EOR can only be applicable for sandstone reservoirs. Low salinity water can change the wettability of sandstone or silicate surfaces toward water-wet conditions and subsequently takes part in crude oil recovery enhancement. On the other hand, according to some other groups, wettability alteration could also be a possible event in carbonate reservoirs by modifying the injection-brine chemistry.[12,17−21]

Apart from the reservoir rock type, the nature of the crude oil present in the reservoir is an important factor affecting the performance of the low salinity-EOR process and needs to be examined carefully. Almost 90% of the low salinity core-flood experiments were performed using medium to slightly heavy crude oil samples.[15,22,23] Moreover, the crude oil used in these studies possesses a high acid number and many of them have not even reported the acid number of the oil they used in their studies.[24−27] Usually, a high acid or base number is found with heavy crude oil which contains fewer lighter components. Tang and Morrow[2] investigated the low salinity waterflooding process for crude oil of 27°API and acid number of 0.33. The study of low salinity by Pu et al.[15] used crude oil ranging from 25 to 31°API with an acid and a base number ranging up to 0.56 and 2.29, respectively. Winoto et al.[23] tested low salinity waterflooding performance using crude oil of API gravity 24° with an acid number of 1.46. Lashkarbolooki et al.[19] have reported a mechanistic investigation of low salinity waterflooding using crude oil of 22°API and an acid number of 1.5. Aslan et al.[17] reported studies on wettability alteration during low salinity waterflooding for crude oil ranging from 21 to 30°API. Researchers have also investigated the effect of asphaltene and resin which is present in the crude oil in varying amounts on the performance of low salinity waterflooding.[28] Therefore, the outcome of various laboratory tests leads to the interpretation that the low salinity-EOR works only for the reservoirs that contain medium gravity oil with a significant polar content such as fatty acids or naphthenic acids. Very limited studies were performed until now using light crude oil and crude with a low acid number.[21,25] Many of the world's large oil reserves are producing crude oil which is light and paraffinic in nature with a low acid and base number. Therefore, it is equally important to understand the applicability and mechanism of the novel low salinity waterflooding process for such light paraffinic low acid number crude oil reservoirs, which might have been different from the high acid number heavy crude oil reservoirs.

The present work investigates the EOR performance of the emerging low salinity-EOR technique for reservoirs containing light paraffinic crude oil with a low acid number. The study has been performed to address the question that whether a high acid number or the presence of polar components in crude oil is an indispensable condition to increase the crude oil recovery using low salinity-EOR. The recovery efficiency was evaluated at high temperature via laboratory flooding experiments using sand packs saturated with seawater as connate brine and crude oil from an offshore oilfield of India. High salinity seawater was injected in each case to replicate the secondary recovery process in order to obtain residual oil saturation as a target for

low salinity-EOR. Subsequently, low salinity waterflooding (with 50, 25, and 10% seawater dilution) was applied as a tertiary recovery method. Indeed, the evaluation of oil recovery efficiency is not the only aspect that is being investigated in this work. Additional investigations include the study on the IFT of crude oil−low salinity water, wettability studies through contact angle measurements, and chemical analysis of the effluent brine produced during the oil recovery process. The study also aims to understand the underlying mechanism responsible for possible physicochemical changes that lead to EOR during low salinity-EOR. Possible mechanisms such as in-situ soap generation and electrical double-layer expansion are explained during interpretation of the obtained results.

2. RESULTS AND DISCUSSION

The oil recovery performance of diluted seawater or low salinity waterflooding, also referred to as low salinity-EOR, over high salinity seawater has been evaluated through laboratory flooding experiments. The results of IFT and wettability studies (via contact angle measurement) have been discussed to understand more insights into the underlying mechanism of the low salinity-EOR process. The effluent brine produced during waterflooding experiments is analyzed to know useful information on the mechanism.

2.1. Effect of Injection-Water Salinity on EOR Performance. In this study, three different low salinity waterflooding experiments have been performed, the detail of which is explained in Experimental Section. The petrophysical properties of the sand packs used for these experiments are reported in Table 1. Table 2 reports the summary on residual

Table 1. Properties of the Sand Packs Used for Different Low Salinity-EOR Experiments

| sand-pack number | porosity (%) | saturation (%) | | k_w in mD (at $S_w = 1$) | k_o in mD (at S_{wi}) |
		S_{wi}	S_{oi}		
1	27.85	29.5	70.48	93.52	13.00
2	28.91	32.11	67.89	71.62	11.39
3	27.32	30.09	69.99	86.31	11.09

oil saturation after secondary and low salinity-EOR, oil recovery efficiencies, and total cumulative oil recovery [% of original oil in place (OOIP)]. Figure 1a−c depicts the cumulative oil recovery percentage (oil recovery efficiency in terms of OOIP) and the pressure drop as a function of the amount of the pore volume (PV) injected. The water cut profiles during the core-flooding experiments have been portrayed in Figure 2a−c.

Figure 1a portrays the recovery factor as a function of the volume of the fluid injected for 50% seawater flood, which is trailed behind a high salinity seawater flood (secondary waterflood). During the high salinity seawater flood (secondary recovery), the crude oil recovery efficiency increases sharply until the first 0.3 PV of injection; thereafter, the oil recovery increases gradually. After 1.5 PV of high salinity seawater injection, the oil production ceased and the recovery efficiency profile (% OOIP) reached a flat plateau. An additional 3.5 PV of seawater is injected to ensure that the oil recovery from high salinity secondary waterflood comes to an end and no mobile oil remains trapped because of the capillary end effect. After a total 5 PV of seawater injection, the flood scheme was switched to 50% seawater (diluted to 50% salinity of original seawater).

Table 2. Results of Seawater and Diluted Seawater Flooding Experiments

| sand-pack number	experiment	S_{oi} (% of PV)	seawater flooding or secondary recovery		low salinity-EOR or tertiary recovery		cumulative oil recovery (% OOIP)
			S_{or} (% of PV)	recovery efficiency (% OOIP)	S_{or} (% of PV)	recovery efficiency (% OOIP)	
1	seawater-50% seawater	70.48	39.86	43.45	38.43	2.03	45.48
2	seawater-25% seawater	67.89	36.60	46.08	31.47	7.57	53.65
3	seawater-10% seawater	69.99	38.20	45.35	35.70	3.58	48.93

During 50% seawater injection, no significant oil production or increase in recovery efficiency has been observed. During the first 1.5 PV of 50% seawater injection, the recovery efficiency slightly increases by an additional of 2.03% OOIP as compared to the secondary recovery (Table 2). The oil recovery at the end of high salinity seawater flood was 43.45% OOIP, which increased to only 45.48% even after the injection of 5 PV of 50% seawater (Table 2). It can also be observed that the injection of 50% seawater has reduced the residual oil saturation only by 1.43%. The water cut during high salinity waterflooding sharply increased to 83% of the total production rate (oil + water) immediately after 0.4 PV of seawater flood (Figure 2a). At the end of 1.6 PV of seawater injection, the water cut has reached to 100% and remained the same until 5 PV of seawater injection. During the last 3.4 PV of seawater injection, the water cut reached to 100%, that is, the production stream contained only water and there were no traces of oil in it. When the injection water was changed to 50% seawater, the water cut dropped to 98% at the beginning but again increased to 100% immediately after 1.4 PV of 50% seawater flooding.

The oil recovery profile during 25% seawater flooding is plotted in Figure 1b. During the secondary recovery or high salinity seawater flooding, the oil recovery has increased sharply to 37% OOIP during first 0.3 PV of seawater injection. After that, the recovery has gradually increased to 46.08% until 1.4 PV of seawater flood. After 1.4 PV, the recovery profile reached a flat plateau and no more oil production was observed until the end of 4 PV seawater injection. The injection rate was bumped between 4 and 5 PV, but no further oil production was observed during the rate bumping. After 5 PV of high salinity seawater flooding, the injection water was changed to 25% seawater injection. As a result of 25% seawater flooding, the oil production was started again and the oil recovery has shown a continuous upraise. The recovery efficiency at the end of 6.5 PV of cumulative water injection was 53.65% OOIP. No further increase in recovery was observed after 6.5 PV of cumulative injection. From Table 2, it can be observed that an additional oil recovery of 7.57% was obtained from 25% seawater flooding over high salinity seawater flood. It can also be noticed from Table 2 that 25% seawater flooding has reduced the residual oil saturation from 36.60 to 31.47% OOIP. Compared to 50% seawater, injection of 25% seawater has significantly improved the oil recovery efficiency and reduces the residual oil saturation that is left after high salinity seawater flooding or secondary recovery. The water cut has followed a similar trend as previously discussed. Figure 2b shows that the water cut increased sharply in the beginning and reached almost 97% after 0.5 PV of seawater injection. Subsequently, it was reduced continuously to 91% at the end of 0.9 PV of seawater injection; however, it again increased to

100% and remained the same until the end of secondary recovery or high salinity seawater injection (until the end of 5 PV cumulative water injection). When 25% seawater was injected, the water cut decreased and showed a fluctuating trend with a minimum value of 89% at 5.8 PV. After that, the water production increased and reached to 100% after 6.6 PV of water injection and remained the same until the end of 10 PV.

Figure 1c shows the oil recovery during 10% seawater flooding following a high salinity seawater flood. The oil recovery percentage has increased rapidly in the beginning up to 0.4 PV and increased further with a gradual trend until 1.7 PV of seawater injection. After that, no oil was recovered from the secondary waterflood. The oil recovery percentage at the end of high salinity seawater flood was 45.35% OOIP (Table 2). Injection of 10% seawater has increased the oil recovery only by 3.58% as compared to high salinity seawater flood (secondary recovery). Figure 2c shows that the water cut rapidly increased in the beginning of high salinity seawater flooding and reached to 98% after approximately 1 PV of seawater injection. Subsequently, during 10% seawater injection, the water cut was reduced to 96% at the beginning but again increased with further injection and reached to 100%. From Table 2, it can be observed that secondary recovery values are almost equal in all three experiments, which represent that the secondary recovery experiments were considerably repeatable. This provides uniform starting conditions (e.g., S_{or} and S_w) for all three low salinity waterflooding experiments, which is a very crucial condition for evaluating or comparing results of any EOR experiment.

Apart from oil recovery and water cut profiles, Figure 1a–c also depicts the pressure drop profiles across the sand pack during seawater and diluted seawater injection. From Figure 1a, it can be observed that the pressure drop across the sand pack during high salinity seawater flooding at a rate of 0.2 mL/min got stabilized at 19 psi. The injection of high salinity water was continued until a stabilized recovery and a stabilized pressure drop profile were obtained. As the flow rate has been increased after 4 PV of seawater injection, the pressure drop profile showed a sharp increase up to 42 psi at about 5 PV. After that, when the injection water was switch to 50% seawater (0.2 mL/min), the pressure drop was observed to be stabilized at a lower value (17.5 psi) as compared to the high salinity seawater flooding (19 psi). The lower stabilized pressure drop during 50% seawater flooding was probably because of the continuous flow of water through the channels that bypassed through the oil zone after breakthrough. During 50% seawater, not much significant oil was displaced from the pores and water moved unrestricted through the channels. This resulted in a lower pressure drop during 50% seawater injection. From Figure 1b, we can observe that during high
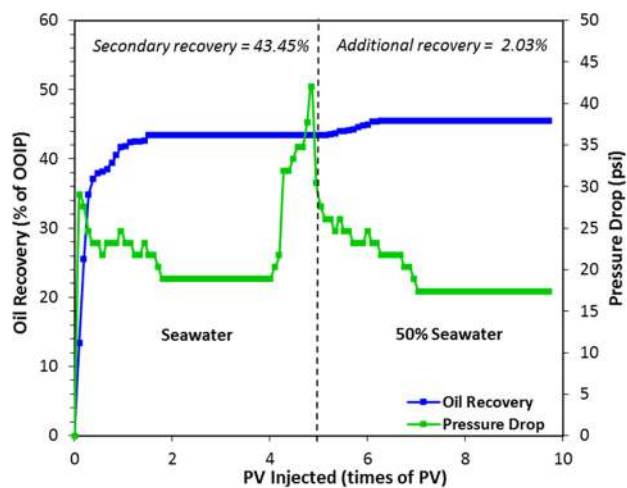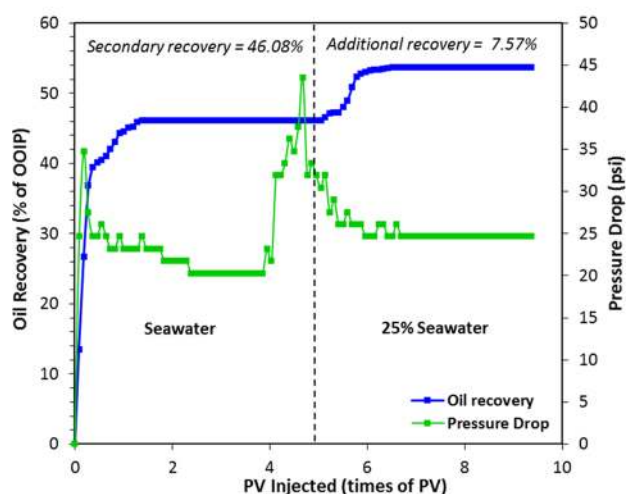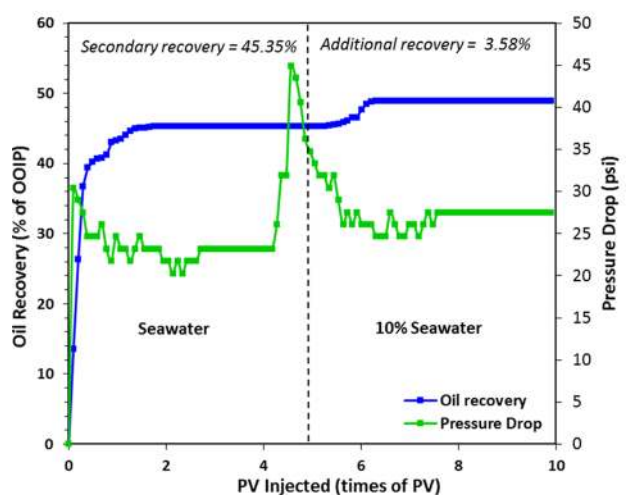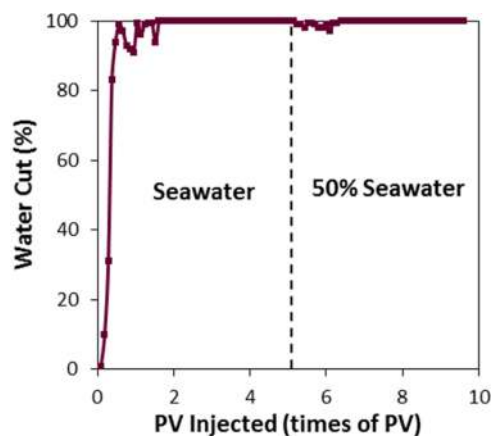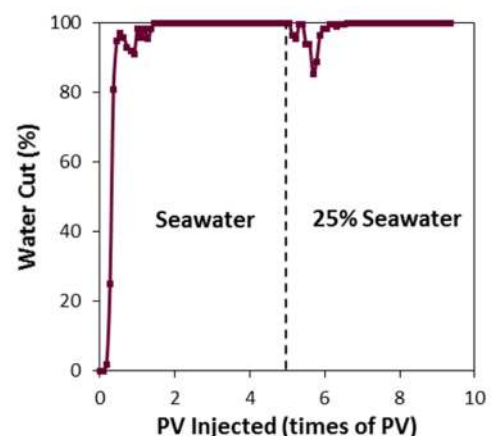
Figure 1. Oil recovery efficiency and pressure drop profile of high and low salinity waterflooding plotted as a function of injected fluid volume in multiples of PV: (a) seawater flooding followed by 50% seawater flooding; (b) seawater flooding followed by 25% seawater flooding; and (c) seawater flooding followed by 10% seawater flooding (each 1 PV on the abscissa contains 10 data points).
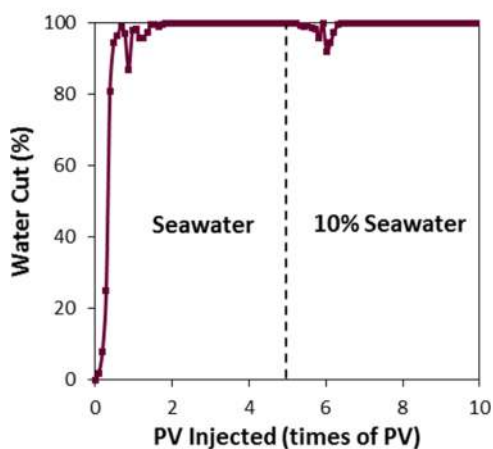

Figure 2. Water cut or the percentage of water in the production stream as a function of PV. (a) Seawater flooding followed by 50% seawater flooding; (b) seawater followed by 25% seawater flooding; and (c) seawater followed by 10% seawater flooding (each 1 PV on the abscissa contains 10 data points).

salinity seawater flooding, the pressure drop profile was stabilized at 20 psi. During the rate bumping, the pressure

drop profile showed an upraise and reached 43.5 psi. During 25% seawater injection, the pressure drop was stabilized at 24.6 psi. The stabilized pressure drop during 25% seawater injection was higher than the high salinity seawater injection. The lower salinity of injection water probably resulted in swelling of the clay present in the sand pack and caused a reduction in permeability. This is one of the reasons why we have observed

a higher pressure drop during 25% seawater injection. Another possible reason that resulted in a higher pressure drop is the redistribution or mobilization of trapped oil because of low salinity water injection. Similarly, from Figure 1c, in the case of 10% seawater flooding, a higher stabilized pressure drop (27.5 psi) was observed as compared to high salinity seawater flood (23 psi). During 10% seawater injection, although additional oil was produced, the additional recovery was not as high as that in the case of 25% seawater injection. The higher pressure drop during 10% seawater injection as compared to its secondary high salinity waterflood was probably attributed to clay swelling than redistribution or mobilization of trapped oil. There might be a possibility that the increased pressure drop results in a better displacement of crude oil through the pore network of reservoir rock during low salinity waterflooding.

Low salinity waterflooding experiments using both sand packs and cores have been reported previously in the literature by various authors.[15,29−31] The incremental recoveries from low salinity laboratory core-flooding experiments are observed to be different by different investigators. Fu[31] evaluated the efficiency of low salinity waterflooding using sand packs and found an additional 15% oil recovery in comparison with high salinity waterflooding. The low salinity waterflood recovery observed by Tang and Morrow[2] was ranged between 1.4 and 5.8%, whereas Pu et al.[15] obtained 5.2−7.2% additional oil recovery by injecting low salinity coal bed methane water in Tensleep and Minneluas sandstone cores. Nasralla et al.[32] reported 14−22% additional oil recovery by injecting deionized water and low salinity aquifer water into Berea sandstone cores. Zhang et al.[33] observed 10−30% incremental oil recovery from low salinity water injection into core samples from the Shengli oilfield. These observations imply that the recovery efficiency of low salinity experiments could be different depending on the type of materials (particularly the core and crude oil) used. However, the additional oil recovery observed in this study using 25% seawater (7.57%) injection is certainly an encouraging result of the low salinity effect.

2.2. Effect of Salinity on IFT. Figure 3 shows different IFT measurements of crude oil with seawater and with different diluted versions of seawater. It can be observed from
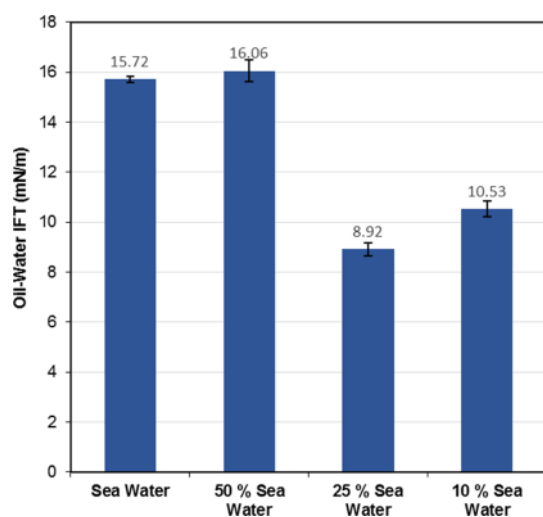

Figure 3. Results of IFT measurements between crude oil and different injection water at 70 °C (IFT values reported are the average of three independent measurements).

the results that the IFT between the crude oil used in this study and high salinity seawater is 15.72 mN/m. Because of the low specific gravity of the crude oil, the IFT is lower than the typical black oil−water IFT. In the case of 50% seawater, the IFT value did not undergo any significant change, as it increased only by 0.34 mN/m. For 25% seawater, the IFT value was decreased to 8.92 mN/m. In the case of 10% seawater, the resulting IFT value was higher than in 25% seawater. The increase in oil recovery with brine dilutions (50, 25, and 10% seawater) is observed to be in line with the IFT results (Figures 1 and 3). The lower IFT at 25 and 10% seawater has probably improved the displacement of crude oil and played a role in enhancing the oil recovery. The trends in IFT values observed in this study are similar to the one observed for a pure alkane−brine system in our previous study.[34] Al-Attar et al.[35,36] have reported crude oil−seawater IFT values for crude oil from the Bu Hasa oilfield and seawater from Arabian Gulf (40 980 ppm). They have observed a continuous increase in IFT with brine dilution. However, there are studies on IFT between crude and diluted formation of water reporting minima in IFT at a particular low salinity concentration.[37,38] Again, some studies also reported IFT minima for crude oil and a single salt brine system.[19,39,40] Although the low salinity concentration corresponding to the minimum IFT is different in our study from the above cited studies, the trends in the reduction of IFT are in line with the reported studies and reflect the implication of low salinity waterflooding. In our previous study[34] on the effect of salt on the IFT of the pure alkane−brine system, we have proposed a mechanism of IFT reduction at low salt concentrations. The reason behind the minimum IFT was explained with the Gibbs adsorption isotherm. Initially, when the salt concentration is low, the dissociated ions in water are preferentially located at or around the hydrocarbon−water interface, even if the bulk concentration is low. The cations get adsorbed at the interface because of the interaction with the hydrocarbon phase either through cation-induced dipole interaction with the nonpolar molecules or interaction with different polar groups in the oil phase. As the ions migrate to the interface, the surface excess turns positive and leads to a reduction in IFT. Therefore, we have observed a decrease in IFT at low salt concentrations. After a certain concentration of the salt, the interface becomes saturated with cations and subsequent addition of salt increases the bulk concentration. As a result, the surface excess decreases and causes an increase in IFT with a minimum IFT value.

2.3. Effect of Salinity on the Contact Angle. Contact angle measurements were performed to address the impact of injection-brine dilution on the wettability of the rock-forming mineral surface. It is considered as one of the most common methods in petroleum research to quantify reservoir rock wettability.[41,42] To interpret wettability regimes from contact angle results, Anderson's[43] classification of wettability is used: from 0 to 75° as water-wet, from 75 to 115° as intermediate-wet, and from 115 to 180° as oil-wet. Figure 4 shows the photographs of the oil droplets in deionized water and seawater at varying temperatures in the range from 25 to 70 °C. It could be observed that the contact angle increases with the increase in the temperature. However, the increase in the contact angle or wettability transition was much more significant when the oil droplet was in a high salinity (seawater) environment. High salinity and high temperature can transform the silicate surface into the oil-wet state. The reason behind such behavior is that with the increase in
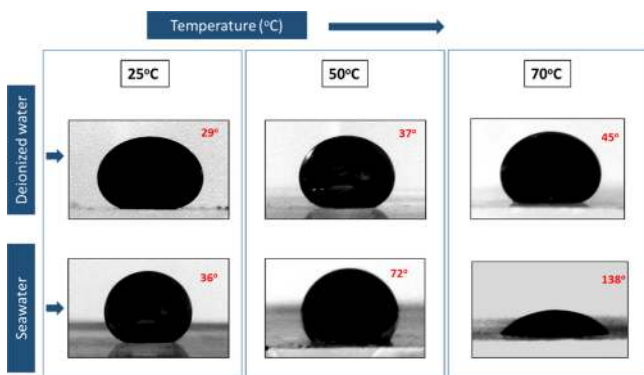
Figure 4. Photographs of the oil droplet in deionized water and high salinity water (seawater) at varying temperatures (25, 50, and 70 °C). The contact angles reported are the average of the right and left contact angle analyzed with ImageJ using DropSnake Plugin. Photograph courtesy of "Ganesh Kumar". Copyright 2019. This image is free domain.

temperature, the thickness of embedding water film between the oil and silicate surface decreases dramatically.[44] The reduction in the thickness of the embedding water film on the silica surface decreases because of the breaking of hydrogen bonds. This in turn causes the silicate surface to shift toward a oil-wet regime because of the thinning of water film.[45] Again, as salinity increases, the amount of the divalent ion also increases which helps in binding the negative charge-bearing molecules of crude oil to the negatively charged silicate surface via the ion-binding mechanism.[46] Figure 5 shows images of the
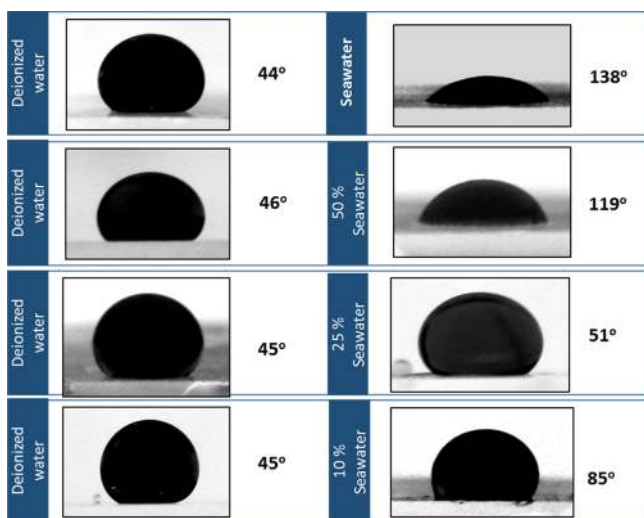

Figure 5. Photographs of the oil droplet in high and low salinity environments at 70 °C. The first row of images represents initial wettability of the substrates measured in deionized water at the same temperature. The contact angles reported are the average of the right and left contact angle analyzed with ImageJ using DropSnake Plugin. Photograph courtesy of "Ganesh Kumar". Copyright 2019. This image is free domain.

oil droplets in different brine environments (high/low salinity). The droplet in the first row represents the initial wetting conditions for each experiment. It can be observed that the initial wetting conditions are reasonably identical for all the experiments. Figure 6 shows the change in contact angle values and the respective wetting regime with varying brine salinities.
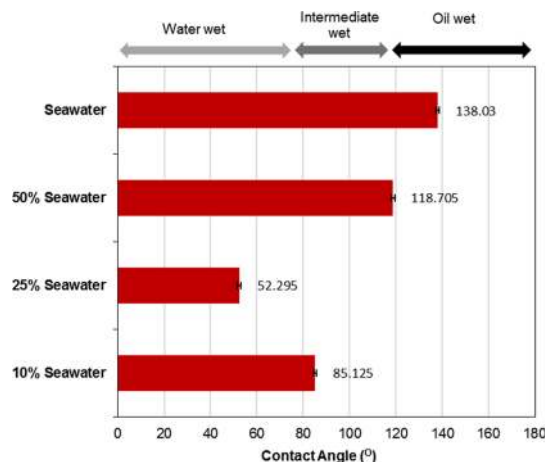

Figure 6. Contact angle values of the oil droplet placed on a quartz substrate surrounded by different injection water at 70 °C (Contact angle values reported are the average of three independent measurements).

From the results, it has been observed that the contact angle with high salinity seawater is 138°, indicating an oil-wet state. When the 50% seawater was used, the contact angle has slightly decreased to 119° but remained in the oil-wet regime. We have observed a significant change in the contact angle with 25% seawater. The contact angle has reduced to 51°, which indicate that the silicate surface is in a water-wet regime in 25% seawater. When 10% seawater was used, the contact angle was observed to be greater than that of 25% seawater (85°), making the silicate surface intermediate-wet. The results indicate that dilution of injection brine or reduction in injection-brine salinity can significantly change the wettability of the rock-forming mineral surface. The highest shift in wettability toward the water-wet state was observed in the case of 25% seawater which is in line with the waterflooding experiments, which also results in the highest additional oil recovery as compared to other low salinity seawater injections. The shift of the wetting state of reservoir rock with altering brine salinity was reported previously in the literature by few authors.[10,47−51] However, contact angle studies using quartz and seawater were not reported previously, instead these were reported for mica surfaces.[32] Alotaibi et al.[47] observed a larger contact angle in the case of high salinity seawater as compared to low salinity aquifer water and deionized water. Aslan et al.[17] observed a nonmonotonous wetting behavior of the quartz surface with varying NaCl and CaCl$_2$ concentrations. For NaCl brine, they observed the most water-wet state within an optimum concentration range of 0.1 and 1 M, and for CaCl$_2$, the optimum concentration range was reported to be within 0.001−0.1 M. The optimum brine concentration range corresponding to the most water-wet state of the silicate surface was found to be different from different studies depending on the type of the crude oil and substrate used. However, one common observation is that the reduction in brine salinity can make the silicate or sandstone surface more water-wet, which is favorable for enhanced waterflood recovery. The explanation for the salinity-dependent contact angle was described in our recent study.[52] The reason behind a minimum contact angle could be related to the IFT through the Young's equation. According to this relation, the reduction in oil−water IFT can result in a lower oil−water−solid contact angle. The reduction in IFT up to an optimum salt

concentration has led to a reduction in the contact angle. The reason is also applicable for the uprising trend of the contact angle after the optimum salt concentration. Apart from that, the reduction in brine salinity also helps in detaching the polar oil components bridged to the mineral surface via ions in the aqueous phase.

2.4. Results of Effluent Brine Analysis. Figure 7 shows variation in pH of the effluent water that is produced during
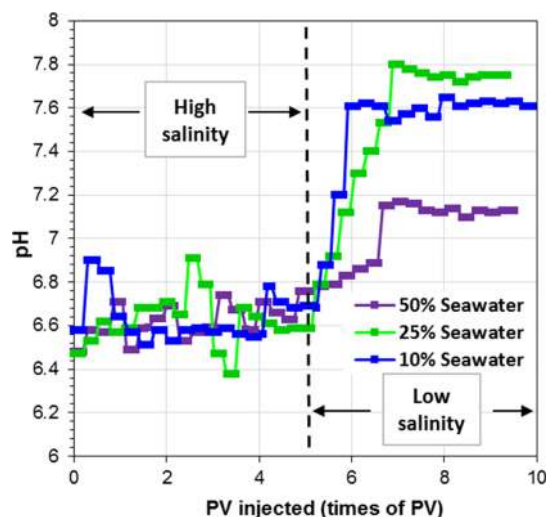

Figure 7. pH of the effluent or produced water during waterflooding plotted as a function of the volume of water injected (measured at intervals of ~0.3 PV).

the waterflooding experiments and is plotted as a function of injected fluid volume for all the flooding experiments carried out in this study. We observe from Figure 7 that the effluent brine during low salinity water injection has a higher pH value as compared to the effluent produced during high salinity seawater flooding in all three core-flooding experiments. Although the increase in pH was observed and is in line with the observation by other researchers,[6,14,53−55] the actual cause behind pH elevation during low salinity water injection is not known. According to Austad et al.[53] the divalent ions that help in binding polar crude oil components to the clay or silicate surface remain in chemical equilibrium during high salinity seawater injection. Injection of low salinity seawater disturbs this chemical equilibrium, and the divalent ions tend to free themselves in order to re-establish the chemical equilibrium. The surrounding water molecules help to facilitate this process by dissociating them into H^+ and OH^- ions. H^+ ions from the water molecules adsorb onto the clay surface because of their high affinity to the clay surface, and the OH^- ions remain in solution resulting in an increase in pH. H^+ ions also adsorb to the clay minerals as a substitute for the divalent ions. This alters the wettability of the rock surface by dissociation of the organo−metallic complexes formed by the crude oil components onto the rock surface via cation-bridging. The elevated pH probably also results in expansion of the electrical double layer which increases water wetness of the reservoir rock surface. In addition, the elevated pH also promotes saponification of the natural surface-active compounds in the crude oil to generate in-situ surfactants. This contributes to the reduction of oil−water IFT. However, in the case of crude oil with a higher acid number, the IFT reduction would have been more prominent as it contains a higher

amount of surface-active compounds. Figure 8 shows the total dissolved solids (TDS) of the effluent water produced during
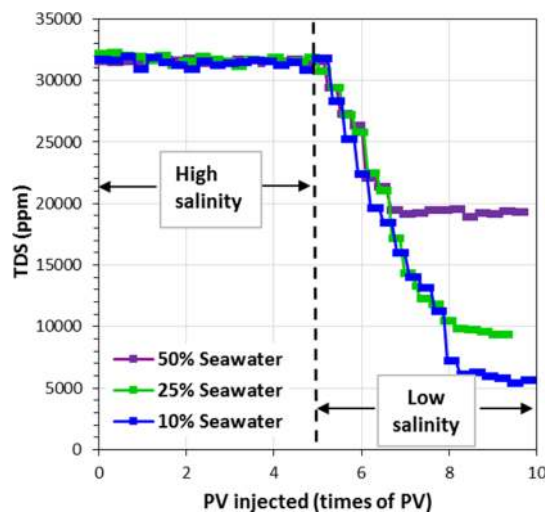

Figure 8. TDS of the effluent or produced water during waterflooding plotted as a function of the volume of water injected (measured at intervals of ~0.3 PV).

waterflooding experiments plotted as a function of the volume of water injected. TDS of the effluent water is an important parameter to evaluate, which gives an insight into the mechanism of low salinity waterflooding. The results show that during low salinity or diluted seawater flooding, TDS of the produced effluent water is higher than the injection-water TDS. For example, in the case of 50% seawater injection, the TDS of the injection water is ~16 000 ppm, but the produced effluent water was found to have a minimum TDS of ~19 000 ppm. Similarly, in the case of 25% seawater, a difference of ~3000 ppm was observed between effluent brine and injection brine. During high salinity seawater injection, the crude oil binds with the pore walls via attractive interaction and bridges by the ions present in the interstitial water. The interstitial water therefore contains a high amount of ions. Low salinity water injection disturbs this association, thereby helping in the release of ions and the attached organic molecules of the crude oil. These ions are released because of the breakdown of the organo−metallic complexes and come out with the effluent water.[14,17,19] This results in a difference in TDS between the effluent and low salinity injection water. The breakdown of the organo−metallic complexes caused by the intrusion of low salinity water is one of the main reasons behind recovery enhancement in low salinity waterflooding.

2.5. Efficiency, Environmental, and Economic Benefits of Low Salinity-EOR. Laboratory core-flooding studies on low salinity waterflooding by various researchers reported varying oil recovery efficiencies depending on the type of the core, crude oil, and brine chemistry employed. The lab-scale additional oil recovery of low salinity-EOR is found to be in the range between 5 and 21% OOIP.[56−58] For example, Austad et al.[53] evaluated low salinity-EOR performance using a sandstone core and obtained an additional oil recovery of 15%. Similarly, Tang and Morrow[22] have obtained 5.8% additional oil recovery from core-flooding experiments using Berea sandstone. Putervold et al.[56] observed an additional oil recovery up to 6% OOIP from low salinity waterflooding for chalk cores. Fathi et al.[57] observed 8−18% additional oil

recovery from their laboratory experiments using chalk cores. Gupta et al.[58] from their low salinity-EOR experiments reported an additional oil recovery of 5.1−21.3% for limestone and dolomite cores. Data available in the literature indicate that the pilot-scale low salinity-EOR operation in some fields reported reduction in the residual oil saturation by 10−24%.[6,8,10,11] This represents that the oil recovery obtained from the lab-scale and pilot-scale low salinity test is in line. In the case of chemical EOR, most laboratory studies show an additional oil recovery of 20−30% OOIP, whereas the field applications show an additional oil recovery of 12−30% OOIP.[59,60] This shows that the efficiency of low salinity-EOR is comparable to that of chemical EOR methods.

There are immense environmental impacts associated with chemical EOR operations. Some of these environmental impacts are as follows: (1) deterioration of the surface water quality due to chemical contamination, (2) contamination of shallow water aquifers, (3) production of toxic and carcinogenic substances from synergistic interactions among chemicals during chemical EOR processes, and (4) loss of biota.[61] The contamination may occur as a result of the spill of chemicals during preparation, transportation through surface lines and storage facilities, failure of injection and the production well, migration through fractures in reservoirs, and so forth. As low salinity waterflooding does not involve the injection of any chemicals and it completely relies on tuning or modification of injection-brine chemistry, there are no or little impacts on the environment. In comparison with chemical EOR, the environmental impact of low salinity-EOR is insignificant, as in the case of waterflooding. As the injection water has a lower salinity, it may not cause significant environmental and ecological imbalance, if in case it gets mixed with groundwater sources.

The economic feasibility of any EOR method is a crucial factor for its successful implementation. Only having a technical ability to increase oil recovery cannot establish it to be an efficient EOR method. The cost of reservoir development using low salinity-EOR primarily depends on the desalination cost. Because a low salinity water source may not be available at all locations, desalination of the formation water or seawater is required in such cases. The cost of desalination cannot be exactly determined because it depends on the time and location. According to an economic evaluation of low salinity-EOR by Althani,[62] the desalination cost could be only 14% of the profit gained from low salinity-EOR. As most of today's oil fields are under waterflooding operations, low salinity-EOR does not require any additional facility for the injection purpose. Although in this study, 5 PV of low salinity water was injected in each case, the incremental oil recovery was observed only during the first 1 PV of low salinity water injection for all the experiments. The additional 4 PV water was injected only to ascertain that no capillary-trapped oil is left in the core. From a field perspective, if we inject low salinity water to recover the residual oil which is left after high salinity waterflooding (rather than applying low salinity waterflooding in a secondary mode), then this will reduce the desalination cost by reducing the amount of low salinity water required. In comparison with chemical EOR methods, low salinity-EOR is much economical as the cost of chemicals in chemical EOR methods is very high. For example, in the case of alkaline-surfactant-polymer flooding, the cost of the chemical could be 10 USD/bbl of incremental oil.[60]

Apart from the low-operating cost, another most important benefit from low salinity-EOR is the reduced risk of corrosion of production facility. The chance of inorganic-scale formation in production installations and also in the reservoir is minimum in low salinity-EOR.

3. CONCLUSIONS

The oil recovery efficiency of the emerging low salinity-EOR method has been tested for light crude oil with a low acid number. Diluted seawater in different proportions was injected in core-flooding experiments to find out the impact of injection-water salinity on oil recovery. In addition, IFT, contact angle measurements, and effluent brine analysis were performed to investigate the mechanism of oil recovery enhancement. Based on the results gathered from this study, the following conclusions can be drawn:

1. The results of waterflooding experiments using a crude oil with a low acid number show that injection of diluted seawater has a significant potential for improving oil recovery as compared to high salinity seawater injection.

2. The highest additional oil recovery is obtained in the case of 25% seawater injection. The impact of 50% seawater injection was negligible, and with 10% seawater injection, the oil recovery has improved but not as significant as the 25% seawater injection case.

3. Low salinity water injection results in a higher pressure drop as compared to the pressure drop during high salinity water injection.

4. Recovery mechanism studies show that dilution of injection water has an obvious impact on oil−water IFT and significantly influences the reservoir rock wettability. At an optimum dilution, a minimum IFT and strongly water-wet condition can be achieved, which results in additional oil recovery from low salinity-EOR.

5. Although pH-induced soap generation could slightly contribute to the low salinity effect in every crude oil type, the primary mechanism of IFT reduction and associated wettability alteration in a low acid number crude oil is attributed to the preferential movement of cations to the oil−water interface.

4. EXPERIMENTAL SECTION

4.1. Materials. The crude oil used for this study was provided by Chennai Petroleum Corporation Limited (CPCL) produced from an offshore oilfield of India. The crude oil properties are listed in Table 3. Figure 9 shows the Fourier transform infrared (FTIR) spectra of the crude oil used in this study. The FTIR report shows that the crude oil contains alkanes, carboxylic functionalities along with a small amount of phenols, and amines. The wide band between 2500 and 3300 cm^{-1} corresponds to carboxylic acid. The band 1400−1500

Table 3. Properties of the Crude Oil Used

properties	values
specific gravity	0.8286
API gravity	39.30
viscosity @40 °C (cSt)	2.70
pour point (°C)	30
sulphur (wt %)	0.12
acid number (mg KOH)	0.12
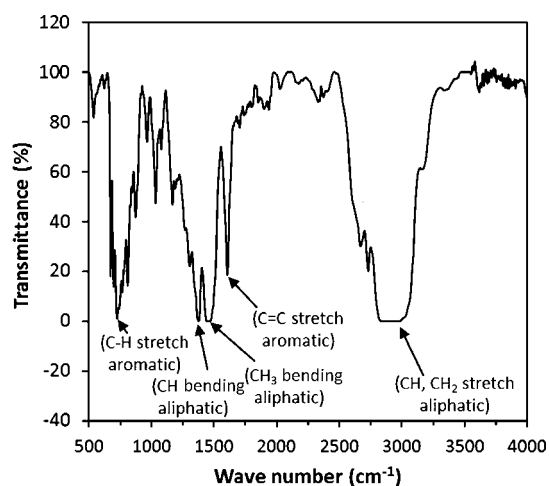
Figure 9. FTIR spectra of the Indian crude oil used in this study.

Figure 10. Schematic diagram of the experimental setup used for waterflooding experiments. Photograph courtesy of "Ganesh Kumar". Copyright 2019. This image is free domain.

cm^{-1} shows that the crude oil also contains some aromatic compounds.[63] The sand used to prepare the sand pack for core-flood experiments is sieved through a mesh of 0.3–0.6 mm. XRD analysis showed that it is composed primarily of silica. Bentonite clay (2 wt %) had been mixed with the sand while preparing the sand pack. This was done in order to simulate more accurate reservoir mineralogy, as actual sandstone reservoirs always contain some amounts of clay, deposited in the geological past along with sediments. The quartz plate for contact angle measurements is purchased from a local vendor in Chennai, India. Deionized water having a resistivity of 18.2 MΩ cm (at 25 °C) from a Milli-Q system (Millipore, U.S.) was used to prepare diluted versions of the high salinity seawater (50, 25, and 10% seawater) which were used as low salinity water. The concentration of the major ions in seawater and their different diluted versions used for injection is reported in Table 4. The ionic concentrations were determined as per the standard procedure given in the "standard methods for the examination of water and wastewater".[64]

Table 4. Ionic Composition of the Different Injection Water Used in This Study

ions	concentration (ppm)			
	seawater	50% seawater	25% seawater	10% seawater
Na^+	11 806	5903	2952	295
Ca^{2+}	1200	600	300	120
Mg^{2+}	3960	1980	990	396
Cl^-	18 197	9099	4549	1820
SO_4^{2-}	2086	1043	522	20
salinity	32 754	16 378	8188	3276
pH	7.23	7.19	7.25	7.15

4.2. Low Salinity-EOR Experiments. Figure 10 shows the experimental setup used for low salinity waterflooding experiments. The setup consists of a sand-pack reactor which has a uniform diameter stainless steel cylindrical tube (diameter: 4 cm and length: 30 cm) surrounded by an integrated water jacket. The reactor was custom-designed and fabricated by D-Cam Engineering, Ahmedabad, India. The flooding experiments were conducted at a high temperature (70 °C) by circulating hot water into the water jacket from a water bath (TC-650, Brookfield, USA) which has an operating
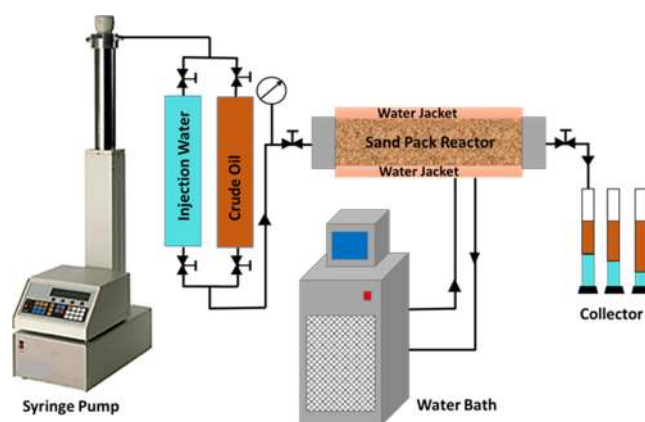
temperature range of −20 to +200 °C. The crude oil and injection water (seawater) are stored in two different accumulator bottles of 500 mL capacity and are made up of stainless steel. A syringe pump (Teledyne ISCO, 500D, USA) with a maximum capacity of 507.3 mL was used to inject various fluids from the accumulators into the sand pack. The oil saturation was achieved by displacing the oil from the accumulator into the sand pack with the help of water from the syringe pump. Water was used in the syringe pump to displace crude oil because it is immiscible with crude oil. Similarly, during waterflooding, the injection water was injected into the sand pack with the help of a hydrocarbon solvent filled in the syringe pump. This procedure was used to ensure the safe operation of the syringe pump. It is to be noted here that the height of the accumulator bottles (Figure 10) is sufficiently high enough as compared to its cross-sectional area, which ensures that the interface of two injection fluids remains stable. Moreover, extreme care has been taken to ensure that the accumulators are sufficiently filled with the injection fluid so that the interface does not go down significantly. Again, the flow rate is very low, which keeps the interface stable and therefore there is no chance of turbulence that can cause mixing of the two fluids. This prevents the pump fluid from entering into the sand pack. The pressure difference across the sand pack was monitored with a digital pressure gauge attached at the inlet of the sand-pack reactor. Because the outlet of the sand pack was at atmospheric pressure, the gauge reading was considered as the pressure drop across the sand pack and the same is used to determine the permeability of the sand pack.

The sand pack was prepared by filling the reactor with silica sand mixed with bentonite clay (2 wt %). The sand used in these experiments was in the size range of 0.3–0.6 mm mesh size. Bentonite clay was mixed with sand to simulate reservoir mineralogy as sandstone reservoirs also contain a small amount of clay. Although the clay content in reservoirs varies over a wide range, in most sandstone reservoirs, it occurs between 2 and 8 wt %.[65] The lowest value in this range (2 wt %) has been taken to avoid permeability damage that could be induced by low salinity water. During its filling, the sand was simultaneously saturated with seawater. The total amount of water required to saturate the sand pack fully was considered as the pore volume (PV) of the sand pack. The bulk volume (BV) of the sand pack is equal to the volume of the reactor cylinder into which sand was filled, which was known from the

reactor dimensions. The porosity is determined as the ratio of PV to BV. After the sand pack was ready, it was flooded with seawater to measure the absolute permeability (k) of the sand pack using Darcy's equation. Five measurement points were recorded at an interval of 0.1 PV for permeability measurement after a stabilized pressure was achieved. The reported permeability is the average of five permeability values. The flow rate was set at 0.5 mL/min during permeability measurements. Once the absolute permeability has been measured, crude oil was injected into the sand pack. As crude oil was injected into the sand pack, the saturated water from the sand pack started to get displaced and is produced at the outlet. A sufficient amount of crude oil was injected even after the water cut or water production stopped from the outlet of the pack. The oil injection rate was varied in order to displace any mobile water that could have been trapped at the outlet because of the capillary end effect. The production stream at this point contains almost only crude oil and further injection of the crude oil into the sand pack could not displace any more water out of the sand pack. At this stage, the water left in the pores of the sand pack is called connate water saturation or irreducible water saturation or initial water saturation. The amount of oil left inside the sand pack was calculated with a simple material balance method. The oil volume remaining inside the sand pack is equal to the amount of water that has come out of the sand pack and is called OOIP. The initial oil saturation (S_{oi}) and initial water saturation (S_{wi}) were calculated as

$$S_{oi} = \frac{OOIP}{PV} \times 100\%$$ (1)

$$S_{wi} = \frac{PV - OOIP}{PV} \times 100\%$$ (2)

Once initial crude oil and connate water saturations were achieved, the sand pack was aged at 70 °C for more than 48 h to establish equilibrium between sand grains, crude oil, and water. Like any other EOR method, low salinity waterflooding also targets the residual oil left after secondary oil recovery. Therefore, the aged sand pack was first flooded with high salinity seawater until the oil production becomes zero or insignificant. In all the flooding experiments performed in this work, approximately 5 PV of high salinity seawater was injected initially in a secondary mode to establish minimum residual oil saturation (S_{or}). The injection scheme during the water-flooding experiments is depicted in Figure 11. The high salinity seawater was injected at a constant rate of 0.2 mL/min, which is equivalent to 2 ft/day for the sand-pack dimension used in this study. In order to mimic the flow rate inside the reservoir during waterflooding operation, a standard flow rate of 2 ft/day is used for our flooding experiments. After 4 PV of the seawater injection, the rate was increased to 0.5, 1, and 2 mL/min during the last 1 PV seawater injection (from 4 to 5 PV). This rate bumping was performed in order to recover any mobile oil that is trapped because of the capillary end effect.

The produced mixture of oil and water was collected in graduated cylinders at an interval of ~0.1 PV (approximately 10 sampling points in 1 PV) and later heated for a sufficiently long time in a water bath for thorough separation of the two phases. The separated volumes of oil and water are noted for the calculation of the oil recovery factor. The sand-pack holder is designed to have a very minimal dead volume for accurate
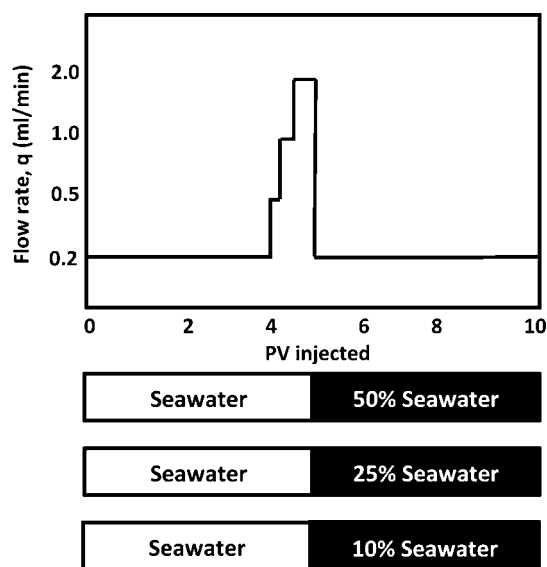

Figure 11. Injection scheme of the low salinity waterflooding experiments.

measurement of the produced fluids and to avoid any production delay. The residual oil saturation was calculated as

$$S_{or} = \frac{OOIP - volume\ of\ oil\ produced}{PV} \times 100\%$$ (3)

Once it has been observed that the production stream contains no traces of crude oil or no further oil production was possible from high salinity seawater flood, the injection scheme was switched to diluted seawater (low salinity water). The low salinity waterflooding has been performed in this work using 50% seawater, 25% seawater, and 10% seawater (low salinity water). The number represents the percentage of seawater in the prepared low salinity injection water. As shown in Figure 11, almost 5 PV of diluted seawater or low salinity water was injected at a rate of 0.2 mL/min (the same as of high salinity seawater injection) in each case of the low salinity water-flooding experiments performed in this work. The oil recovery efficiency after each low salinity-EOR experiments has been calculated using eq 4

$$Oil\ recovery\ efficiency = \frac{volume\ of\ oil\ produced}{OOIP} \times 100\%$$ (4)

The details are discussed in Results and Discussion.

4.3. IFT Measurements. The IFT between crude oil and different diluted versions of seawater was measured by the Wilhelmy plate method. A dynamic contact angle tensiometer (DCAT 11 EC, Dataphysics, Germany) was employed to perform the IFT measurements using a PT 11 Wilhelmy plate (Dataphysics, Germany). Figure S1 (in the Supporting Information) shows the experimental setup used for IFT measurements. The instrument offers an accuracy of approximately ±0.01 mN/m. The temperature of the fluids under investigation was maintained by circulating hot water from a water bath (IC 201, Escy Enterprises, Pune, India) into the water jacket integrated with the sample holder in the tensiometer. However, the sample temperature was measured and confirmed with a built-in temperature sensor which has an accuracy of ±0.1 K. More detailed information on the experimental procedure is reported in our previous work.[34,52]

4.4. Contact Angle Measurements. The contact angle measurements were performed in order to assess if there is any wettability change associated with seawater dilution or salinity reduction. A quartz substrate with a smooth surface was used for these studies as a representative of the sandstone or silicate mineralogy. To measure the contact angle, the inverted sessile drop technique was utilized with a custom-made setup, as shown in Figure S2 (in the Supporting Information). The setup comprises a double-walled cylindrical glass cell with an annular space through which water from a water bath (IC 201, Escy Enterprises, Pune, India) was circulated to maintain the experimental temperature (70 °C). The glass cell has a planer quartz window glass in order to capture images of the droplets. The experimental setup and procedures used for cleaning the quartz substrate were reported in our previous work.[66] The substrate has been aged in the high salinity brine first. After that, the substrate was placed in the respective low salinity brine and subsequently the oil droplet was placed below the substrate. Once the oil droplet was placed, the entire system was left undisturbed for 48 h to attain equilibrium. A crude oil droplet (approximately 50 μL) is injected below the substrate with the help of a J-shape needle fitted with a syringe. The droplet moves from the needle tip to the substrate because of the difference in the density of oil from that of the aqueous phase. The images of the droplets were taken with a high-resolution camera (Canon 600D) through a quartz window. The analysis of the drop images is then performed using a Java-based program called ImageJ with a plugin that utilizes the DropSnake method developed by Biomedical Imaging Group at EPFL, Switzerland.[67,68] The average of the left and right contact angle was considered to interpret wettability regimes. More detailed information on contact angle measurements is reported in our previous publication.[66] Identical wetting conditions are important for comparing results of wettability studies. In this study, the initial wetting conditions of the quartz substrates are the same as they are prepared from the same specimen and an identical cleaning procedure and similar aging conditions were applied. To confirm the initial wetting conditions, the substrate wettability is assessed first with deionized water.

4.5. Effluent Brine Analysis. The pH and TDS of the effluent brine produced during waterflooding were analyzed to get more insight of the physicochemical changes that could happen during low salinity water injection. These measurements were done using a Eutech PC 2700 pH/conductivity meter (Thermo Fisher Scientific, Singapore). For pH measurements, the instrument has an operating range of −2.00−20.00 pH and an accuracy of ±0.002 pH. It can measure TDS in the range of 0.050 to 5 00 000 ppm with an accuracy of ±1%.

ASSOCIATED CONTENT

ⓈI Supporting Information

The Supporting Information is available free of charge at https://pubs.acs.org/doi/10.1021/acsomega.9b03229.

    Photograph of the experimental setup used for IFT measurements and schematic of the experimental setup used for contact angle measurements (PDF)

AUTHOR INFORMATION

Corresponding Author

    Jitendra S. Sangwai − *Indian Institute of Technology Madras, Chennai, India;* ⓘ orcid.org/0000-0001-8931-0483; Phone: +91-44-2257-4825; Email: jitendrasangwai@iitm.ac.in; Fax: +91-44-2257-4802

Other Authors

    Abhijit Kakati − *Indian Institute of Technology Madras, Chennai, India*

    Ganesh Kumar − *Indian Institute of Technology Madras, Chennai, India*

Complete contact information is available at:
https://pubs.acs.org/10.1021/acsomega.9b03229

Notes
The authors declare no competing financial interest.

ACKNOWLEDGMENTS

REFERENCES

(1) Austad, T. Water-based EOR in Carbonates and Sandstones: New Chemical Understanding of the EOR Potential Using Smart Water. In *EOR Field Case Studies*; Sheng, J. J., Ed.; Elsevier: Waltham, MA, USA, 2013; Chapter 13, pp 301−335.

(2) Tang, G. Q.; Morrow, N. R. Influence of Brine Composition and Fines Migration on Crude Oil/Brine/Rock Interactions and Oil Recovery. *J. Pet. Sci. Eng.* **1999**, *24*, 99−111.

(3) Jadhunandan, P. P.; Morrow, N. R. Effect of Wettability on Waterflood Recovery for Crude-Oil/Brine/Rock Systems. *SPE Reservoir Eng.* **1995**, *10*, 40−46.

(4) Morrow, N. R.; Tang, G. Q.; Valat, M.; Xie, X. Prospects of Improved Oil Recovery Related to Wettability and Brine Composition. *J. Pet. Sci. Eng.* **1998**, *20*, 267−276.

(5) Tang, G. Q.; Morrow, N. R. Salinity, Temperature, Oil Composition, and Oil Recovery by Waterflooding. *SPE Reservoir Eng.* **1997**, *12*, 269−276.

(6) McGuire, P. L.; Chatham, J. R.; Paskvan, F. K.; Sommer, D. M.; Carini, F. H. Low Salinity Oil Recovery: An Exciting New EOR Opportunity for Alaska's North Slope. Presented at *SPE Western Regional Meeting*: Irvine, California, 30 March−1 April, 2005.

(7) Robertson, E. Low-salinity Waterflooding to Improve oil recovery—Historical Field Evidence. Presented at *SPE Annual Technical Conference and Exhibition*: Anaheim, California, U.S.A., 11−14 Nov, 2007.

(8) Seccombe, J. C.; Lager, A.; Webb, K. J.; Jerauld, G.; Fueg, E. Improving Waterflood Recovery: LoSaltm EOR Field Evaluation. Presented at *SPE Symposium on Improved Oil Recovery*: Tulsa, Oklahoma, USA, 20−23 April, 2008.

(9) Skrettingland, K.; Holt, T.; Tweheyo, M. T.; Skjevrak, I. Snorre Low-Salinity-Water injection—Core Flooding Experiments and Single-Well Field Pilot. *SPE Reservoir Eval. Eng.* **2011**, *14*, 182−192.

(10) Vledder, P.; Gonzalez, I. E.; Fonseca, J. C.; Wells, T.; Ligthelm, D. J. Low Salinity Waterflooding: Proof of Wettability Alteration on a Field Wide Scale. Presented at *SPE Improved Oil Recovery Symposium*: Tulsa, Oklahoma, USA, 24−28 April, 2010.

(11) Webb, K. J.; Black, C. J. J.; Al-Ajeel, H. Low Salinity Oil Recovery—Log-Inject-Log. Presented at *SPE Middle East Oil Show*: Bahrain, 9−12 June, 2003.

(12) Yousef, A. A.; Liu, J.; Blanchard, G.; Al-saleh, S.; Al-zahrani, T.; Al-zahrani, R.; Al-Tammar, H. Smart Waterflooding: Industry's First Field Test in Carbonate Reservoirs. Presented at *SPE Annual Technical Conference and Exhibition*: San Antonio, Texas, USA, 8−10 October, 2012.

(13) Boussour, S.; Cissokho, M.; Cordier, P.; Bertin, H.; Hamon, G. Oil Recovery by Low Salinity Brine Injection: Laboratory Results Outcrop and Reservoir Cores. Presented at *SPE Annual Technical Conference and Exhibition*: New Orleans, Louisiana, 4−7 October, 2009.

(14) Lager, A.; Webb, K. J.; Black, C. J. J.; Singleton, M.; Sorbie, K. S. Low Salinity Oil Recovery—An Experimental Investigation. *Petrophysics* **2008**, *49*, 28−35.

(15) Pu, H.; Xie, X.; Yin, P.; Morrow, N. R. Low Salinity Waterflooding and Mineral Dissolution. Presented at *SPE Annual Technical Conference and Exhibition*: Florence, Italy, 19−22 September, 2010.

(16) Tang, G.; Morrow, N. M. Oil Recovery by Waterflooding and Imbibition—Invading Brine Cation Valency and Salinity. *Proceedings of the International Symposium of the Society of Core Analysts*: Golden, CO, August 1999.

(17) Aslan, S.; Najafabadi, N. F.; Firoozabadi, A. Non-Monotonicity of the Contact Angle from NaCl And $MgCl_2$ Concentrations in Two Petroleum Fluids on Atomistically Smooth Surfaces. *Energy Fuels* **2016**, *30*, 2858−2864.

(18) Hognesen, E. J.; Strand, S.; Austad, T. Waterflooding of Preferential Oil-Wet Carbonates: Oil Recovery Related to Reservoir Temperature and Brine Composition. Presented at *SPE Europec/EAGE Annual Conference*: Madrid, Spain, 13−16 June, 2005.

(19) Lashkarbolooki, M.; Ayatollahi, S.; Riazi, M. The Impacts of Aqueous Ions on Interfacial Tension and Wettability of an Asphaltenic—Acidic Crude Oil Reservoir during Smart Water Injection. *J. Chem. Eng. Data* **2014**, *59*, 3624−3634.

(20) Sharma, G. Wettability Alteration in High Temperature and High Salinity Carbonate Reservoirs. Presented at *SPE Annual Technical Conference and Exhibition*: Denver, Colorado, USA, 30 October−2 November, 2011.

(21) Romanuka, J.; Hofman, J.; Ligthelm, D. J.; Suijkerbuijk, B.; Marcelis, F.; Oedai, S.; Brussee, N.; van der Linde, H.; Aksulu, H.; Austad, T. Low salinity EOR in Carbonates. Presented at *SPE Improved Oil Recovery Symposium*: Tulsa, Oklahoma, USA, 14−18 April, 2012.

(22) Suleimanov, B. A.; Latifov, Y. A.; Veliyev, E. F.; Frampton, H. Comparative Analysis of the EOR Mechanisms by Using Low Salinity and Low Hardness Alkaline Water. *J. Pet. Sci. Eng.* **2018**, *162*, 35−43.

(23) Winoto, W.; Loahardjo, N.; Morrow, N. R. Assessment of Oil Recovery by Low Salinity Waterflooding from Laboratory Tests. Presented at *SPE Improved Oil Recovery Symposium*: Tulsa, Oklahoma, USA, 12−16 April, 2014.

(24) AlQuraishi, A. A.; Alhussinan, S. N.; Alyami, H. Q.; Abdulaziz, K. Efficiency and Recovery Mechanisms of Low Salinity Waterflooding in Sandstone and Carbonate Reservoirs. Presented at *12th Offshore Mediterranean Conference and Exhibition*: Ravenna, Italy, 25−27 March, 2015.

(25) Cissokho, M.; Boussour, S.; Cordier, P.; Bertin, H.; Hamon, G. Low Salinity Oil Recovery on Clayey Sandstone: Experimental Study. *Petrophysics* **2010**, *51*, 305−313.

(26) Liu, Y.; Jiang, T.; Zhou, D.; Zhao, J.; Xie, Q.; Saeedi, A. Evaluation of the Potential of Low Salinity Waterflooding in the High Temperature and High Salinity Dong-He-Tang Reservoir in the Tarim Oilfeild, China: Experimental and Reservoir Simulation Results. Presented at *SPE Asia Pacific Oil & Gas Conference and Exhibition*: Perth, Australia, 25−27 October, 2016.

(27) Mohsenzadeh, A.; Pourafshary, P.; Al-Wahaibi, Y. Oil Recovery Enhancement in Carbonate Reservoirs via Low Saline Waterflooding in Presence of Low Concentration Active Ions; A Case Study. Presented at *SPE EOR Conference at Oil and Gas West Asia*: Muscat, Oman, 21−23 March, 2016.

(28) Garcia-Olvera, G.; Reilly, T. M.; Lehmann, T. E.; Alvarado, V. Effects of Asphaltenes and Organic Acids on Crude Oil-Brine Interfacial Visco-Elasticity and Oil Recovery in Low-Salinity Waterflooding. *Fuel* **2016**, *185*, 151−163.

(29) Ebrahim, T.; Mohsen, V. S.; Mahdi, S. M.; Esmaeel, K. T.; Saeb, A. Performance of Low-Salinity Water Flooding for Enhanced Oil Recovery Improved by SiO_2 nanoparticles. *Pet. Sci.* **2019**, *16*, 357−365.

(30) Ding, Y.; Zheng, S.; Meng, X.; Yang, D. Low Salinity hot Water Injection with Addition of Nanoparticles for Enhancing Heavy Oil Recovery under Reservoir Conditions. *J. Energy Resour. Technol.* **2019**, *141*, 072904.

(31) Fu, J. Y. A study of low salinity water flooding in 1D and 2D. MS Thesis, The University of Texas at Austin, 2011.

(32) Nasralla, R. A.; Bataweel, M. A.; Nasr-El-Din, H. A. Investigation of Wettability Alteration and Oil-Recovery Improvement by Low-Salinity Water in Sandstone Rock. *J. Can. Pet. Technol.* **2013**, *52*, 144−154.

(33) Zhang, L.; Zhang, J.; Wang, Y.; Yang, R.; Zhang, Y.; Gu, J.; Zhang, M.; Ren, S. Experimental Investigation of Low-Salinity Waterflooding in a Low-Permeability Oil Reservoir. *Energy Fuels* **2018**, *32*, 3108−3118.

(34) Kakati, A.; Sangwai, J. S. Effect of Monovalent and Divalent Salts on the Interfacial Tension of Pure Hydrocarbon-Brine Systems Relevant For Low Salinity Waterflooding. *J. Pet. Sci. Eng.* **2017**, *157*, 1106−1114.

(35) Al-Attar, H. H.; Mahmoud, M. Y.; Zekri, A. Y.; Almehaideb, R.; Ghannam, M. Low-Salinity Flooding in a Selected Carbonate Reservoir: Experimental Approach. *J. Pet. Explor. Prod. Technol.* **2013**, *3*, 139−149.

(36) Al-Attar, H. H.; Mahmoud, M. Y.; Zekri, A. Y.; Almehaideb, R. A.; Ghannam, M. T. The Impact of Losal on Oil Recovery from a Selected Carbonate Reservoir in Abu Dhabi—An Experimental Approach. Presented at *SPE Middle East Oil and Gas Show and Conference*: Manama, Bahrain, 10−13 March, 2013.

(37) Vijapurapu, C. S.; Rao, D. N. Compositional Effects of Fluids on Spreading, Adhesion and Wettability in Porous Media. *Colloids Surf., A* **2004**, *241*, 335−342.

(38) Okasha, T. M.; Al-Shiwaish, A. J. Effect of Brine Salinity on Interfacial Tension in Arab-D Carbonate Reservoir, Saudi Arabia. Presented at *SPE Middle East Oil & Gas Show and Conference*: Bahrain, 15−18 March, 2009.

(39) Moeini, F.; Hemmati-Sarapardeh, A.; Ghazanfari, M.-H.; Masihi, M.; Ayatollahi, S. Towards Mechanistic Understanding of Heavy Crude Oil/Brine Interfacial Tension: The Role of Salinity, Temperature and Pressure. *Fluid Phase Equilib.* **2014**, *375*, 191−200.

(40) Manshad, A. K.; Olad, M.; Taghipour, A. S.; Nowrouzi, I.; Mohammadi, A. H. Effects of Water Soluble Ions on Interfacial Tension (IFT) Between oil and Brine in Smart and Carbonated Smart Water Injection Process in Oil Reservoirs. *J. Mol. Liq.* **2016**, *223*, 987−993.

(41) Pal, N.; Vajpayee, M.; Mandal, A. Cationic/Nonionic Mixed Surfactants as Enhanced Oil Recovery Fluids: Influence of Mixed Micellization and Polymer Association on Interfacial, Rheological, and Rock-Wetting Characteristics. *Energy Fuels* **2019**, *33*, 6048−6059.

(42) Kumar, A.; Mandal, A. Critical Investigation of Zwitterionic Surfactant for Enhanced Oil Recovery from both Sandstone and Carbonate Reservoirs: Adsorption, Wettability Alteration and Imbibition Studies. *Chem. Eng. Sci.* **2019**, *209*, 115222.

(43) Anderson, W. G. Wettability Literature Survey- Part 1: Rock/Oil/Brine Interactions and the Effects of Core Handling on Wettability. *J. Pet. Technol.* **1986**, *38*, 1125−1144.

(44) Derjaguin, B. V.; Churaev, N. V. On the Question of Determining the Concept of Disjoining Pressure and Its Role in the Equilibrium and Flow of Thin Films. *J. Colloid Interface Sci.* **1978**, *66*, 389−398.

(45) Punase, A.; Zou, A.; Elputranto, R. How Do Thermal Recovery Methods Affect Wettability Alteration? *J. Pet. Eng.* **2014**, *2014*, 538021.

(46) Buckley, J. S.; Liu, Y.; Monsterleet, S. Mechanism of Wetting Alteration by Crude oils. *SPE J.* **1998**, *3*, 54−61.

(47) Alotaibi, M.; Nasralla, R.; Nasr-El-Din, H. Wettability Studies Using Low-Salinity Water in Sandstone Reservoirs. *SPE Reservoir Eval. Eng.* **2011**, *14*, 713.

(48) Agbalaka, C. C.; Dandekar, A. Y.; Patil, S. L.; Khataniar, S.; Hemsath, J. R. Core Flooding Studies to Evaluate the Impact of Salinity and Wettability on Oil Recovery Efficiency. *Transp. Porous Media* **2009**, *76*, 77−94.

(49) Strand, S.; Puntervold, T.; Austad, T. Effect of Temperature on Enhanced Oil Recovery from Mixed-Wet Chalk Cores by Spontaneous Imbibition and Forced Displacement Using Seawater. *Energy Fuels* **2008**, *22*, 3222−3225.

(50) RezaeiDoust, A.; Puntervold, T.; Strand, S.; Austad, T. Smart Water as Wettability Modifier in Carbonate and Sandstone: A Discussion of Similarities/Differences in the Chemical Mechanisms. *Energy Fuels* **2009**, *23*, 4479−4485.

(51) Myint, P. C.; Firoozabadi, A. Thin Liquid Films in Improved Oil Recovery from Low-Salinity Brine. *Curr. Opin. Colloid Interface Sci.* **2015**, *20*, 105−114.

(52) Kakati, A.; Sangwai, J. S. Wettability Alteration of Mineral Surface During Low-Salinity Waterflooding: Role of Salt Type, Pure Alkanes, and Model Oils Containing Polar Components. *Energy Fuels* **2018**, *32*, 3127−3137.

(53) Austad, T.; Rezaeidoust, A.; Puntervold, T. Chemical Mechanism of Low Salinity Waterflooding in Sandstone Reservoirs. Presented at *SPE Improved Oil Recovery Symposium*: Tulsa, Oklahoma, USA, 24−28 April, 2010.

(54) Almeida, A.; Patel, R.; Arambula, C.; Trivedi, J.; Soares, J.; Costa, G.; Embiruçu, M. Low Salinity Water Injection in a Clastic Reservoir in Northeast Brazil: An Experimental Case Study. Presented at *SPE Trinidad and Tobago Section Energy Resources Conference, Port of Spain*: Trinidad and Tobago, 25−26 June, 2018.

(55) Almeida da Costa, A.; Jaeger, P.; Santos, J.; Soares, J.; Trivedi, J.; Embiruçu, M.; Meyberg, G. The Influence of Rock Composition and pH on Reservoir Wettability for Low Salinity Water-CO EOR Applications in Brazilian Reservoirs. Presented at *SPE Annual Technical Conference and Exhibition*: Calgary, Alberta, Canada, 30 September−2 October, 2019.

(56) Puntervold, T.; Strand, S.; Austad, T. Coinjection of Seawater and Produced Water to Improve Oil Recovery from Fractured North Sea Chalk Oil Reservoirs. *Energy Fuels* **2009**, *23*, 2527−2536.

(57) Fathi, S. J.; Austad, T.; Strand, S. Water-Based Enhanced Oil Recovery (EOR) by "Smart Water": Optimal Ionic Composition for EOR in Carbonates. *Energy Fuels* **2011**, *25*, 5173−5179.

(58) Gupta, R.; Smith, G. G.; Hu, L.; Willingham, T.; Cascio, M. L.; Shyeh, J. J.; Harris, C. R. Enhanced Waterflood for Carbonate Reservoirs—Impact of Injection Water Composition. Presented at *SPE Middle East Oil and Gas Show and Conference*: Manama, Bahrain, 25−28 Sept, 2011.

(59) Kamal, M. S.; Hussein, I. A.; Sultan, A. S. Review on Surfactant Flooding: Phase Behaviour, Retention, IFT, and Field Applications. *Energy Fuels* **2017**, *31*, 7701−7720.

(60) Pope, G. A. Recent Developments and Remaining Challenges of Enhanced Oil Recovery. *J. Pet. Technol.* **2011**, *63*, 65−68.

(61) Zoveidavianpoor, M.; Jalilavi, M. Qualitative Analysis of Enhanced Oil Recovery: Impacts on Air, Surface Water and Groundwater. Presented at *International Conference on Chemical, Environment & Biological Sciences (CEBS-2014)*: Kuala Lumpur, Malaysia, 17−18, September, 2014.

(62) Altani, M. An Evaluation of Low Salinity Waterflooding in Carbonates Using Simulation and Economics. MS Thesis, Colorado school of Mines, 2007.

(63) Segneanu, A. E.; Gozescu, I.; Dabici, A.; Sfirloaga, P.; Szabadai, Z. Organic Compounds FT-IR Spectroscopy. In *Macro to Nano Spectroscopy*; Uddin, J., Ed.; Intech Open: London, 2012; Chapter 9, pp 145−164.

(64) Rice, E. W.; Baird, R. B.; Eaton, A. D. *Standard Methods for the Examination of Water and Waste Water*, 22nd ed.; American Public Health Association, American Water Works Association, Water Environment Federation, 2017.

(65) Sayyouh, M. H.; Dahab, A. S.; Omar, A. E. Effect of Clay Content on Wettability of Sandstone Reservoirs. *J. Pet. Sci. Eng.* **1990**, *4*, 119−125.

(66) Kakati, A.; Sangwai, J. S. Wettability Alteration of Mineral Surface During Low-Salinity Waterflooding: Role of Salt Type, Pure Alkanes, and Model Oils Containing Polar Components. *Energy Fuels* **2018**, *32*, 3127−3137.

(67) Stalder, A. F.; Kulik, G.; Sage, D.; Barbieri, L.; Hoffmann, P. A Snake-Based Approach to Accurate Determination of both Contact Points and Contact Angles. *Colloids Surf., A* **2006**, *286*, 92−103.

(68) Williams, D. L.; Kuhn, A. T.; Amann, M. A.; Hausinger, M. B.; Konarik, M. M.; Nesselrode, E. I. Computerised Measurement of Contact Angles. *Galvanotechnik* **2010**, *101*, 2502−2512.